Development 134, 2639-2649 (2007) doi:10.1242/dev.002485

Cohesin-dependent regulation of Runx genes

Julia A. Horsfield[1,*], Sasha H. Anagnostou[1], Jimmy Kuang-Hsien Hu[1,†], Kitty Hsiao Yu Cho[1], Robert Geisler[2], Graham Lieschke[3], Kathryn E. Crosier[1] and Philip S. Crosier[1,‡]

Runx transcription factors determine cell fate in many lineages. Maintaining balanced levels of Runx proteins is crucial, as deregulated expression leads to cancers and developmental disorders. We conducted a forward genetic screen in zebrafish for positive regulators of *runx1* that yielded the cohesin subunit *rad21*. Zebrafish embryos lacking Rad21, or cohesin subunit Smc3, fail to express *runx3* and lose hematopoietic *runx1* expression in early embryonic development. Failure to develop differentiated blood cells in *rad21* mutants is partially rescued by microinjection of *runx1* mRNA. Significantly, monoallelic loss of *rad21* caused a reduction in the transcription of *runx1* and of the proneural genes *ascl1a* and *ascl1b*, indicating that downstream genes are sensitive to Rad21 dose. Changes in gene expression were observed in a reduced cohesin background in which cell division was able to proceed, indicating that cohesin might have a function in transcription that is separable from its mitotic role. Cohesin is a protein complex essential for sister chromatid cohesion and DNA repair that also appears to be essential for normal development through as yet unknown mechanisms. Our findings provide evidence for a novel role for cohesin in development, and indicate potential for monoallelic loss of cohesin subunits to alter gene expression.

KEY WORDS: Runx1, Runx3, Rad21, Scc1, Cohesin

INTRODUCTION

Runx proteins form part of complexes called core binding factors (CBFs); multi-lineage transcriptional regulators with roles in both proliferation and differentiation. CBFs act as dimers that incorporate one of three distinct DNA-binding α subunits (Runx1, Runx2 or Runx3) plus a common non-DNA-binding CBFβ subunit. The Runx component specifies the biological activity of CBF; Runx1 is an essential regulator of hematopoiesis, Runx2 is involved in osteogenesis, and Runx3 is important in neurogenesis and gastric epithelial cell growth control (Blyth et al., 2005; Ito, 2004). Deregulation of Runx function is commonly associated with disease. For example, Runx1 is involved in several chromosomal translocations underlying human leukemias. In addition, changes in the dose of *Runx1* can contribute to neoplasia (Blyth et al., 2005). An important route toward understanding the pathology of Runx-mediated cancers is the elucidation of factors that control either the expression of Runx genes, or the activity/stability of their protein products.

In early zebrafish embryogenesis, *runx1* is expressed in two discrete hematopoietic regions; the anterior lateral-plate mesoderm (ALM), which generates primitive myeloid cells, and the posterior lateral-plate mesoderm (PLM) from which primitive erythroid cells develop (Hsia and Zon, 2005). By around 18 hours post-fertilization (h.p.f.), cells in the PLM have migrated medially to form a central rod of hematopoietic precursors: the intermediate cell mass (ICM). Hematopoietic expression of *runx1* is downregulated in all but the most posterior cells of the ICM at 21 h.p.f., and subsequently reappears in definitive hematopoietic precursors in the ventral wall of the dorsal aorta by 24 h.p.f. (Kalev-Zylinska et al., 2002). *runx1* is also expressed in Rohon-Beard (RB) mechanosensory neurons and in specific neuronal cells (Kalev-Zylinska et al., 2002).

Studies in zebrafish (Burns et al., 2005; Gering and Patient, 2005) and mice (Nakagawa et al., 2006) have shown that *Runx1* is a transcriptional target of Notch signaling during definitive hematopoiesis. In zebrafish, Hedgehog signaling is required for the migration of hematopoietic progenitors to the midline, and for the subsequent formation of *runx1*$^{+}$ definitive precursors (Gering and Patient, 2005). Early PLM *runx1* expression appears to be downstream of a Hox pathway regulated by *caudal*-related homeobox genes *cdx1a* and *cdx4* (Davidson et al., 2003; Davidson and Zon, 2006). In addition the timely initiation (but not maintenance) of *runx1* expression depends on the transcription factors Scl and Lmo2 (Patterson et al., 2007; Patterson et al., 2005). Other factors known to contribute to Runx gene regulation include the BMP signaling pathway (Pimanda et al., 2007), and epigenetic modifications, such as promoter methylation (Lau et al., 2006; Mueller et al., 2007).

To search for potential regulators of *runx1* expression in zebrafish, we conducted an in situ hybridization-based haploid genetic screen of F1 females carrying mutations generated by ethylnitrosourea (ENU). We isolated a mutant, termed nz171, which lacks some neuronal, and all hematopoietic *runx1* expression in early embryogenesis. Through a positional cloning and candidate gene approach, we determined that the gene underlying nz171 was *rad21*, an integral subunit of mitotic cohesin.

Cohesin is a protein complex composed of four major subunits: SMC1, SMC3, RAD21 and SA1 (or SA2), which interact to form a giant ring-like structure. Mitotic cohesin acts as a 'molecular glue' to hold replicated sister chromatids together until the onset of anaphase (Losada and Hirano, 2005; Nasmyth and Haering, 2005). Cohesin also has a DNA repair function (Watrin and Peters, 2006). Intriguingly, it seems that cohesin has additional non cell cycle-related functions (Dorsett, 2007; Hagstrom and Meyer, 2003). In *Drosophila*, loss of Nipped-B, a protein that loads cohesin onto chromosomes, affects expression of the *cut* gene (Dorsett et al.,

[1]Department of Molecular Medicine and Pathology, School of Medical Sciences, The University of Auckland, Private Bag 92019, Auckland, New Zealand. [2]Max Planck Institute für Entwicklungsbiologie, Spemannstrasse 35/III, 72076 Tübingen, Germany. [3]Cancer and Haematology Division, The Walter and Eliza Hall Institute of Medical Research, 1G Royal Parade, Parkville, Victoria 3050, Australia.

*Present address: Department of Pathology, Dunedin School of Medicine, The University of Otago, P.O. Box 913, Dunedin, New Zealand
†Present address: Department of Genetics, Harvard Medical School, 77 Avenue Louis Pasteur, Boston, MA 02115, USA
‡Author for correspondence (e-mail: ps.crosier@auckland.ac.nz)

Accepted 21 May 2007

2005; Rollins et al., 2004). The human ortholog of Nipped-B/Scc2 is NIPBL, and mutations in the *NIPBL* gene, or in the cohesin subunit *SMC1*, underlie the dominant developmental syndrome, Cornelia de Lange (CdLS) (Dorsett, 2007; Musio et al., 2006; Strachan, 2005). Although cohesin clearly has a role in development as well as in the cell cycle, the mechanisms underlying its developmental function are unknown.

Our study provides the first evidence of cohesin-dependent gene regulation in a vertebrate. We found that Runx gene expression depends on the function of the whole cohesin complex and that, as expected, loss of zebrafish cohesin subunits interferes with sister chromatid cohesion during mitosis. Differentiated blood cells were deficient in nz171 mutants, and we found that some of these cells could be rescued by microinjection of *runx1*. nz171 mutants also had neuronal defects and *rad21* was robustly expressed in specific regions of the brain at 48 h.p.f., which might indicate a role in neuronal development. We observed a potent dosage effect of Rad21 on downstream gene expression, and determined that halving the dose of the *rad21* gene reduces the expression of *runx1* and proneural genes *ascl1a* and *ascl1b*. Our findings highlight a new role for cohesin in gene expression and development.

MATERIALS AND METHODS

ENU mutagenesis, mapping and mutant identification

Zebrafish were maintained as described previously (Westerfield, 1995). AB strain males were mutagenized with four treatments of 2.5 mM ENU as described previously (Pelegri, 2002), and were bred with AB females to obtain F1 fish. Eggs from F1 females were fertilized in vitro with UV-irradiated sperm to produce haploid progeny (Pelegri, 2002), which were subjected to in situ hybridization with a *runx1* riboprobe. The nz171 F1 female carrier was crossed to the WIK strain for meiotic mapping. Chromosome localization of the nz171 mutation was performed as described previously (Geisler, 2002). 'Z marker' PCR primer sequences were obtained from the WashU Zebrafish Genome Resources Project (http://zfish.wustl.edu/) and subsequent mapping was performed as described by Geisler (Geisler, 2002).

The genomic sequence of zebrafish *rad21* is available in Ensembl (gene ID ENSDARG00000006092). For mutation analysis, *rad21* was amplified in overlapping segments from cDNA made from 100 pooled nz171 homozygous mutant embryos and 100 wild-type AB embryos (48 h.p.f.). Primers used were Forward-1, 5′-TTCAATGAGAGGAAACGGTTGC-3′; Reverse-1, 5′-ATGATGTCACTGTAGGGCTCGG-3′; Forward-2, 5′-TTCAATGAGAGGAAACGGTTGC-3′; Reverse-2, 5′-GGAAGAGGCTGGTCAAAATCG-3′; Forward-3, 5′-CCCACTTCGTCCTCAGTAAACG-3′; Reverse-3, 5′-TGGTCTTGCTGTCCAACTCCTTC-3′; Forward-4, 5′-AGACAACCGTGAGGCAGCATAC-3′; Reverse-4, 5′-AGTGGAGTCAAGCAGCGAGTAAAC-3′; Forward-5, 5′-ATGTGGAAGGAGACTGGAGGTGTG-3′; Reverse-5 5′-TACAATGTGGAAGCGTGGTCCC-3′; Forward-6, 5′-TCAGGACCAAGAGGAGAGAAGGTG-3′; Reverse-6, 5′-CAACAAGTAGTGAAACTGCGGAGTC-3′. Amplified fragments were cloned and sequenced, and the coding region mutation at nucleotide 829 was represented by two independent overlapping clones and fourfold sequence coverage.

In situ hybridization and histology

In situ hybridization was performed as described previously (Kalev-Zylinska et al., 2002). Embryos to be sectioned were dehydrated in an ethanol series, embedded in JB-4 (Polysciences), cut to a thickness of 5 μm and stained with Giemsa (BDH).

Cell cycle procedures

Bromodeoxyuridine (BrdU) incorporation was performed on whole embryos as described previously (Shepard et al., 2004). Mouse monoclonal anti-BrdU antibody (Zymed) was detected using a Vectastain ABC Kit (Vector Laboratories). Phosphorylated histone H3 was detected as described previously (Shepard et al., 2004). TUNEL staining was performed using the ApopTag Kit from Chemicon as described previously (Shepard et al., 2004).

Microinjection

Full-length zebrafish and human *rad21* clones (RZPD) were subcloned into pCS2$^+$. Amplified full-length *rad21*^{G277X} was subcloned using a ZeroBluntTOPO Kit (Invitrogen), sequenced entirely to confirm the mutation, and subcloned into pCS2$^+$. mRNAs for microinjection were generated using a mMessage mMachine Kit (Ambion), and 100 pg of each was injected into nz171 mutant and sibling embryos at the 1-cell stage. Full-length zebrafish *runx1* in pCS2$^+$ (Kalev-Zylinska et al., 2002) was transcribed as above and 200 pg was injected as above. Morpholino oligonucleotides were obtained from GeneTools LLC and diluted in water. For microinjection, 2 nl of morpholino was injected into the yolk of wild-type embryos from the 1- to 4-cell stages. Morpholino oligonucleotides targeting *rad21* were: *rad21*UTRMO, 5′-CACTACACCTGGAAGAAAACAG-3′; *rad21*ATGMO 5′-TCCTGCTTCACCCGCATTTTGTAAC-3′ (start codon underlined); *rad21*Splx3MO 5′-GATACAATACCTGGGCGGAAAG-3′ (targets 3′ donor of exon 3). Morpholino oligonucleotides targeting *smc3* were *smc3*UTRMO, 5′-GCACAAAACACTCCTCAGAAAC-3′; *smc3*ATGMO, 5′-TGTACATGGCGGTTTATGC-3′ (start codon underlined); *smc3*Splx1MO, 5′-GTGAGTCGCATCTTACCTG-3′ (targets 3′ donor of exon 1) and *smc3*Splx5MO, 5′-TTTCTTACTGGAAGTCTGTTGTCAG-3′ (targets 3′ donor of exon 5). All morpholinos were effective over the range of 0.5-3.0 pmol injected.

Immunofluorescence and confocal microscopy

For immunofluorescence, embryos were fixed and stained with anti-Rad21 (Chemicon International) 1:100, anti-α-tubulin (Sigma-Aldrich) 1:500, and DAPI as described previously (Shepard et al., 2004). FITC- or TRITC-conjugated secondary antibodies (Sigma, 1:500) were used. Flat-mounted samples were imaged using a Leica TCS SP2 confocal microscope.

Quantitative immunoanalysis and quantitative RT-PCR

For immunoblotting, embryos were deyolked in Ringer's solution with EDTA and PMSF, and 20 μg total protein was loaded per lane. For embryos under 12 h.p.f., entire single, or pools of up to 10 embryos were lysed in loading buffer. Sample processing and immunoblotting was performed as described previously (Westerfield, 1995) using anti-Rad21 (Chemicon, 1:500), or anti-α-tubulin (Sigma, 1:2000). Horseradish peroxidase-linked secondary antibodies (Sigma, 1:2000) and enhanced chemiluminescence were used according to the manufacturer's instructions (ECL Plus, Amersham Biosciences, Inc.). Signals were analyzed using Fuji LAS-3000 imager and Fuji Image Gauge software. For quantitative PCR, total RNA from pools of 30-100 embryos was extracted using Trizol (Invitrogen), DNAse-treated, and used to synthesize random-primed cDNA (Invitrogen, SuperScript III). SYBR green PCR Master Mix (Applied Biosystems) was used to amplify cDNA, and relative start quantities were normalized to *β-actin* and *wnt5a* expression. Samples were analyzed using an Applied Biosystems Sequence Detection System 7900HT. Primers for quantitative PCR were designed using the Primer Express program (Applied Biosystems). Sequences are: *runx1* forward, 5′-AGACGTCTCCATCCTGGTCGTA-3′, reverse, 5′-CCGTCAGCTCTGGACAGTGTAA-3′; *rad21* forward, 5′-CAGCATACAATGCCATCACCTT-3′, reverse, 5′-ATTCAGGGTGAACTGCTGTGCTA-3′; *ascl1a* forward, 5′-GGGCTCATACGACCCTCTGA-3′, reverse, 5′-TCCCAAGCGAGTGCTGATATTT-3′; *ascl1b* forward, 5′-CCACATGGTTCGACAGATACGA-3′, reverse, 5′-CAGCATGCAGCAAATCAAAGAC-3′; *β-actin* 5′-CGAGCAGGAGATGGGAACC-3′, reverse, 5′-CAACGGAAACGCTCATTGC-3′; *wnt5a* forward, 5′-GTTCGGCCGCGTCATG-3′, reverse, 5′-TCGACTCACAGCATTCACAACA-3′.

RESULTS

Loss of early *runx1* and *runx3* expression in the zebrafish ENU mutant, nz171

The nz171 mutant was isolated in a haploid in situ hybridization screen because of a marked lack of *runx1* expression in the PLM in early embryogenesis, and lack of blood at 48 h.p.f. In nz171 diploids, *runx1* expression was confirmed lost from the ALM and PLM, but was retained in a subset of RB neurons at the 14-somite stage (Fig. 1A,G compared with D). The *runx3* gene is expressed in

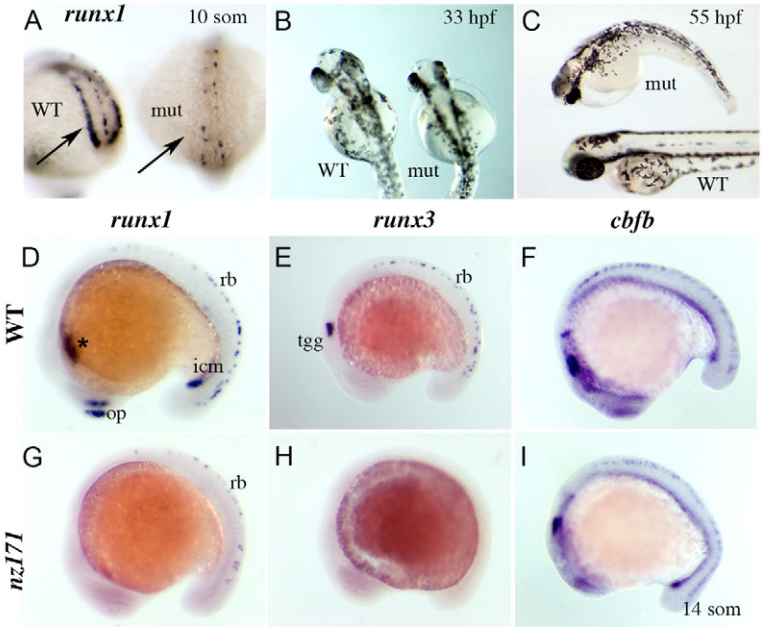

Fig. 1. Zebrafish nz171 homozygous mutants lack *runx1* and *runx3* expression, but retain normal expression of *cbfb*. (**A-C**) *runx1* expression and morphology of nz171 mutants. (A) Loss of *runx1* expression in the PLM (posterior lateral-plate mesoderm; arrows) of an nz171 mutant embryo (mut) compared with wild-type sibling (WT); posterior views of 10-somite embryos. (B,C) Morphology of nz171 mutant (mut) embryos compared with siblings (WT) at the stages indicated (B, dorsal; C, anterior to the left). (**D-I**) Expression of *runx1*, *runx3*, and *cbfb* in wild-type and nz171 mutant embryos (14-somite embryos, anterior to the left). In nz171 mutants, expression of *runx1* is lost in the ICM (intermediate cell mass; icm), ALM (anterior lateral-plate mesoderm; *) and olfactory placode (op) but retained in a subset of the Rohon-Beard (RB) mechanosensory neurons (rb) (G compared with D, wild type). nz171 mutants lack all *runx3* expression (H compared with E, wild type). *cbfb* expression is normal in nz171 mutants (I compared with F, wild type).

a subset of RB cells and in the trigeminal ganglia (TGG) during early embryogenesis (Kalev-Zylinska et al., 2003) (Fig. 1E). Strikingly, its expression was completely absent in nz171 mutants at the 14-somite stage (Fig. 1H). Although both *runx1* and *runx3* are downregulated in nz171, their common binding partner, *cbfb* was expressed normally in neuronal and hematopoietic tissues in equivalent embryos (Fig. 1I compared with 1F). This indicates that the cell types that would normally express *runx1* and *runx3* are present, and that loss of *runx1* and *runx3* expression was not due to gross developmental defects. Early neurogenesis was abnormal in nz171 embryos; the TGG failed to develop properly (although they are specified), and the number of RB neurons was reduced by 30-40% (data not shown). Furthermore, although genes that mark blood vessel formation were expressed (see Fig. S1 in the supplementary material), no visible circulation developed. From the 20-somite stage, nz171 embryos started to exhibit developmental delay, which became increasingly apparent until homozygotes arrested in development at around 35 h.p.f. (Fig. 1B,C). nz171 embryos develop no further, and die at around 3 days postfertilization.

Developmental delay in nz171 mutants is due to a block in mitosis

Giemsa-stained sections of nz171 mutants at the 20-somite stage and older revealed cells that contained abnormal condensed chromosomes, consistent with abnormal mitoses (Fig. 2G,H). To test whether developmental arrest in nz171 mutants is caused by a defect in cell division, we monitored cells in S phase with BrdU incorporation, and cells in M phase with an antibody to phosphorylated histone H3 (pH3). We found no significant difference in the number of cells in S phase between wild-type siblings and nz171 mutants (Fig. 2A,B); however, there were many more cells in mitosis. Cells in M phase started to accumulate from the 14-somite stage, well before a developmental delay is evident (Fig. 2C,D). By the 20-somite stage, there was a marked overrepresentation of cells in M phase in nz171 mutant embryos (Fig. 2E,F). These results are consistent with a block at M phase, in which nz171 mutant embryos take longer to complete mitosis and eventually arrest with all cells blocked in M phase. Giemsa staining of sections revealed that chromosomes in developmentally arrested embryos are condensed and disorganized (Fig. 2G,H). High power microscopy of $pH3^+$ cells indicated that the condensed, disorganized chromosomes are mitotic (Fig. 2H-J). Cells arrested in mitosis probably undergo apoptosis, as revealed by TUNEL. Cell death was particularly prevalent in the ICM and nervous system (Fig. 2K,L).

nz171 embryos have a nonsense mutation in the *rad21* gene

We mapped the nz171 mutation to chromosome 16 between simple sequence length polymorphism (SSLP) markers z25049 and z51029 (Fig. 3A). The cohesin subunit *rad21* also maps to this region, and because of the observed mitotic defect, it was a strong candidate gene for the mutation. *rad21* cDNA was isolated from nz171 homozygotes, sequenced, and a mutation identified in the coding region of the gene (nucleotide 829, exon 8) changing codon 277 from GGA, specifying glycine, to the stop codon TGA (G277X) (Fig. 3B and see Fig. S2 in the supplementary material). An antibody directed against the C-terminal region of human RAD21 detected a specific band in wild-type, but not in mutant embryos (Fig. 3C). An insertional mutant previously mapped to the *rad21* locus (Amsterdam et al., 2004) has a severe early embryonic phenotype (ZFIN ID: ZDB-LOCUS-041006-4) similar to that of nz171, consistent with these defects affecting the same gene.

In wild-type embryos, *rad21* mRNA was detected by RT-PCR at the oocyte stage (Fig. 3D), indicating that the transcript is maternally deposited. Whole-mount in situ hybridization analysis showed that *rad21* was expressed throughout the embryo in early embryogenesis (Fig. 3E,F; data also available on ZFIN, http://zfin.org/). Expression in the brain and posterior tail regions at 26 h.p.f. was particularly robust, most likely because these are areas of active cell division. By contrast, *rad21* transcription was dramatically downregulated in nz171 mutants (Fig. 3E, Fig. 8D), probably owing to nonsense-mediated mRNA decay (Chang et al., 2007). At 48 h.p.f., *rad21* was strongly expressed in discrete areas of the brain, the mandibular cartilage and branchial arches, the otic vesicle and developing pectoral fins (Fig. 3F). Although some cells in these regions would be proliferating rapidly (e.g. the pectoral fins) it is surprising that this expression pattern is so specific. This might reflect a tissue-specific function for Rad21 that is not related to the cell cycle.

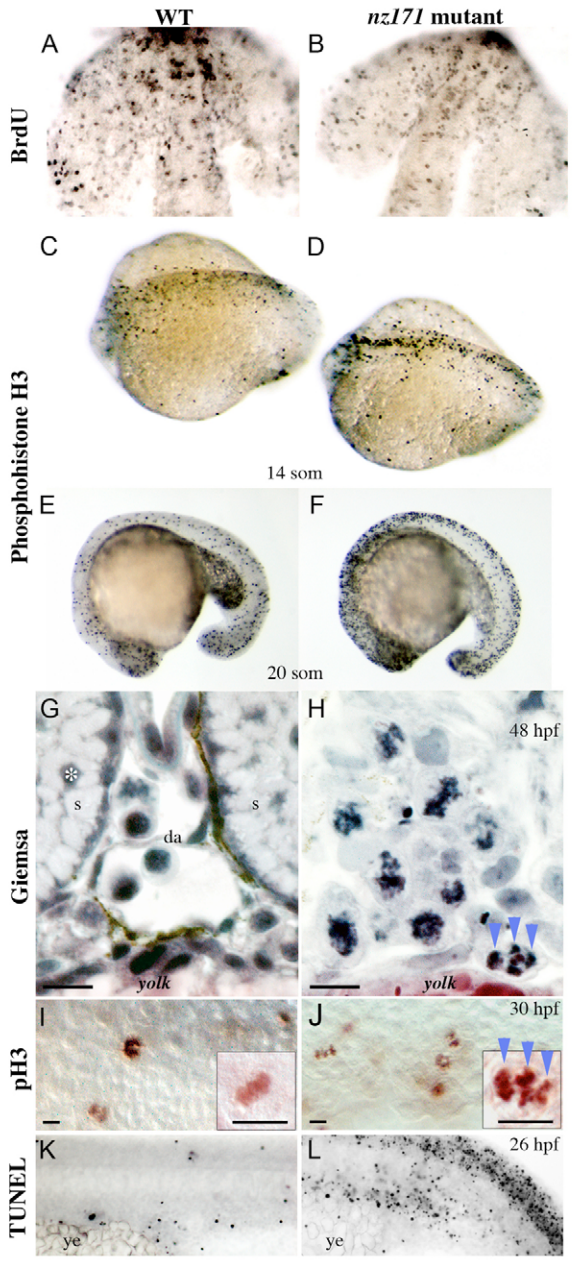

Fig. 2. Cell cycle status of zebrafish nz171 mutant embryos compared with wild-type siblings. (**A**,**B**) BrdU-labeling to detect cells in S-phase in forebrain and eyes of flat-mounted 18-somite embryos, anterior to top. (**C-F**) Dorsal (C,D) and lateral (E,F) views of anti-phosphohistone H3 (pH3)-labeling to detect cells in M phase at the stages indicated (anterior to the left). (**G-J**) Disordered mitotic chromosomes in nz171 mutants. (G,H) Transverse sections bisecting the yolk extension of wild-type (G) and nz171 mutant (H) embryos stained with Giemsa (dorsal to top). Whereas recognizable structures (s, somite; da, dorsal aorta) and normal nuclei (example marked by asterisk) are visible in wild-type embryos, no such structures are visible in nz171 mutants, which have abnormal nuclei with condensed, disorganized chromosomes. pH3-labeled chromosomes of a similar configuration to H (blue arrowheads) appear in nz171 (J) but not in wild-type (I); lateral flat-mounted embryos, mid-trunk (high magnification inset). Scale bar: 20 μm. (**K**,**L**) TUNEL labeling indicates prevalent cell death in the ICM and neuronal regions of nz171 embryos; lateral views of tail regions, anterior to the left, showing the ICM region just above the yolk extension (ye).

To provide further evidence that we had found a mutation in zebrafish *rad21*, we designed antisense morpholino oligonucleotides (MOs) directed against the *rad21* transcript (see Fig. S2 in the supplementary material). MO-injected embryos (termed 'morphants') phenotypically resembled nz171 mutants, had excess pH3^{+} cells and showed dramatic reduction in hematopoietic *runx1* expression (Fig. 4A-I,M). Furthermore, we were able to rescue nz171 mutants with *rad21* mRNA: nz171 mutants approached wild-type morphology at 48 h.p.f. following injection of zebrafish *rad21* mRNA (Fig. 4J,K). In addition, hematopoietic *runx1* expression was rescued (Fig. 4N compared with L), as were mitoses (see Table S1 in the supplementary material; data not shown). By contrast, *rad21* mRNA containing the G277X mutation (*zrad21*^{G277X}) was unable to rescue nz171 mutants (see Table S1 in the supplementary material). Significantly, *runx1* expression was also rescued by human *RAD21* mRNA (Fig. 4O and see Table S1 in the supplementary material), indicating conservation of Rad21 function in both the cell cycle and gene expression through evolution. These results provide conclusive evidence that the nz171 mutation affects the *rad21* locus. We have named our mutant allele *rad21*^{nz171} accordingly.

Although *rad21*^{nz171} mutants lack hematopoietic *runx1* expression, most other early hematopoietic transcription factors are expressed normally

Initial experiments revealed that *runx1* expression in *rad21*^{nz171} mutants was absent from the ALM and PLM. To determine the exact nature of the *runx1* expression defect, we performed a time-course analysis of *runx1* expression in *rad21* morphant and *rad21*^{nz171} mutant embryos (Fig. 5). We found that *runx1* expression was never initiated in the PLM of morphants and mutants (Fig. 5A), but was still expressed in most RB cells (Fig. 5A,B, Fig. 6A). *runx1* mRNA was also deficient in the ALM of *rad21*^{nz171} mutants, although the occasional *runx1*-positive cell was found (Fig. 5C). Loss of *rad21* did not prevent later initiation of neuronal *runx1* expression, as evidenced by expression of *runx1* in neuronal regions of 28 h.p.f. *rad21*^{nz171} mutants (although at reduced levels compared with wild type; Fig. 5D). Since the dorsal aorta does not form in *rad21*^{nz171} mutants (Fig. 2H), later expression of *runx1* there could not be assessed.

In early *rad21*^{nz171} embryos, we observed normal expression of many other early transcription factors essential for hematopoiesis, such as *cbfb* (Fig. 1I) *scl* (also known as *tal1* – ZFIN) and *pu.1* (also known as *spi1* – ZFIN) (Fig. 6A,B), *cmyb*, *cebpa*, *drl* and *gata2* (see Fig. S1 in the supplementary material). The only other early hematopoietic transcription factor affected in *rad21*^{nz171} was *gata1*, which is reduced to about half its normal expression in 10-somite embryos (Fig. 6A). A time-course analysis of *gata1* expression revealed that its onset is slightly delayed in *rad21*-compromised embryos, with levels consistently reduced during early embryogenesis (see Fig. S3 in the supplementary material). This might, at least in part, be due to the positive autoregulation of *gata1* (Kobayashi et al., 2001) by a transcriptional regulatory complex that also contains Runx1 (Elagib et al., 2003; Waltzer et al., 2003).

Normal expression of early blood markers in *rad21*^{nz171} embryos occurred at the same stage that *runx1* expression is lost. Therefore, loss of *runx1* is not due to a developmental delay, or loss of hematopoietic precursors in the regions where *runx1* is normally expressed.

Markers of differentiated blood cells are reduced or absent in *rad21*^{nz171}

In contrast to markers of early hematopoiesis, we determined that later expressed markers, such as *cebpg*, *lyz*, *hbbe3* (Fig. 6C,D), *lcp1* and *mpx* (data not shown) were severely reduced or entirely absent

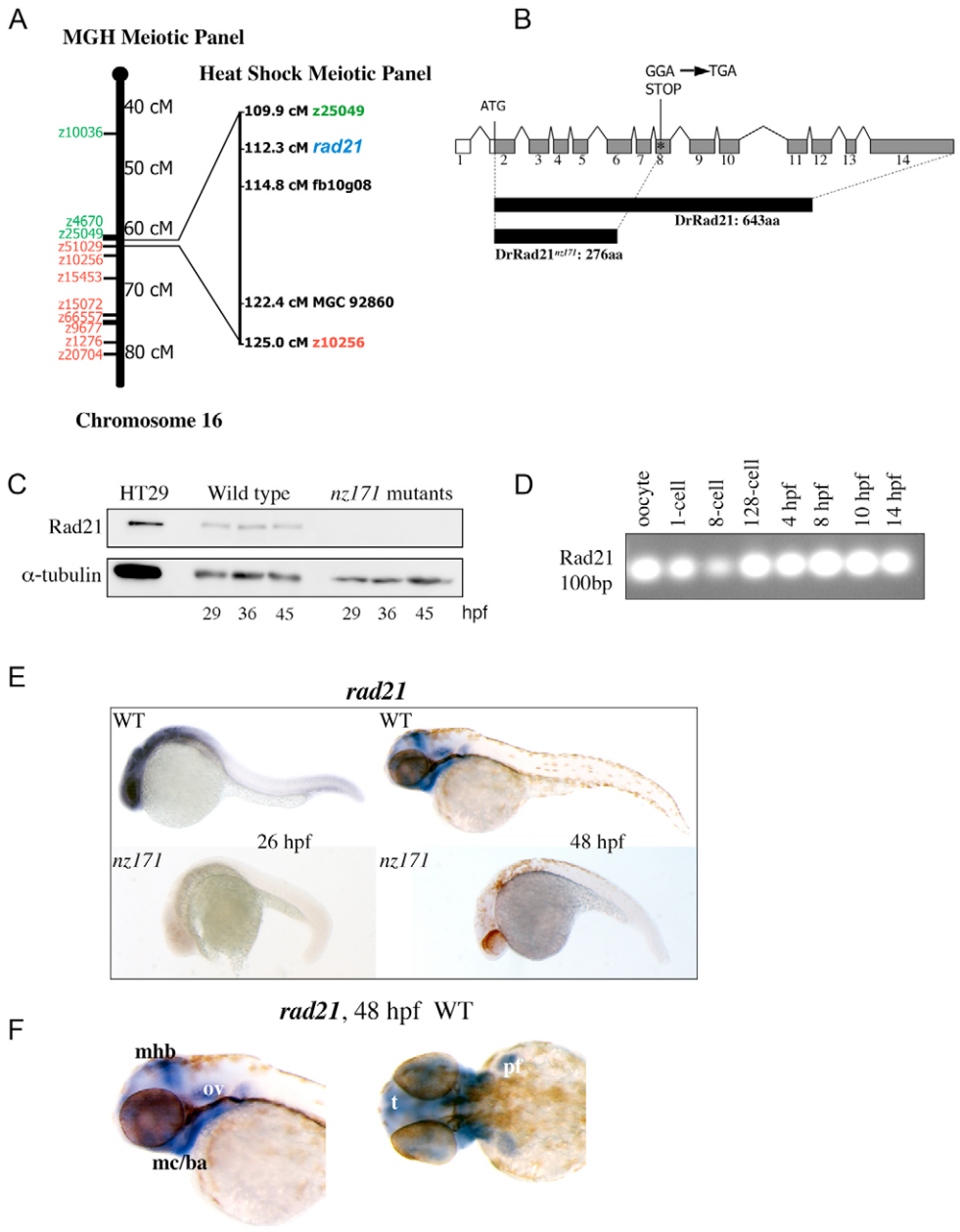

Fig. 3. The nz171 mutation affects the zebrafish *rad21* gene. (**A**) nz171 maps to a region on chromosome 16 containing *rad21*. Schematic of chromosome 16 from the centromere 'southwards', cM (centiMorgans) indicated as per the MGH Meiotic Mapping Panel (http://zebrafish.mgh.harvard.edu/). SSLP markers determined to be 'north' of the mutation are indicated in green and 'south' markers in red. Right, expansion of the interval shown as mapped on the Heat Shock Meiotic panel (Woods et al., 2000) on which nearest north and south markers are shown. The *rad21* gene is shown in blue. (**B**) Schematic representation of the *rad21* gene, coding region shaded gray. A truncated protein is produced as a result of the Gly-277-STOP mutation in exon 8 (asterisk). (**C**) Rad21 protein is not present in nz171 homozygote embryos. Immunoblot showing Rad21 protein and α-tubulin loading control. Positive control is 5 μg protein isolated from HT29 colon carcinoma cells. (**D-F**) *rad21* transcription in wild-type and nz171 embryos. (D) RT-PCR with *rad21*-specific primers indicates *rad21* transcript is maternally inherited in zebrafish embryos. PCR products separated by agarose gel electrophoresis. (E,F) Expression pattern of *rad21* in whole-mount wild-type and nz171 embryos at stages indicated (anterior to the left). *rad21* transcript is undetectable in nz171 mutants (E, lower panels). (F) Lateral (left) and dorsal (right) views of anterior regions showing specific wild-type expression of *rad21* (mhb, midbrain-hindbrain boundary; mc/ba, mandibular cartilage/branchial arches; ov, otic vesicle; t, telencephalon; pf, pectoral fin).

in 24 h.p.f. *rad21*^{nz171} mutants. A summary of the blood defects present in *rad21*^{nz171} is shown in Fig. S1 (see Fig. S1 in the supplementary material). Injection of 200 pg *runx1* mRNA into *rad21*^{nz171} homozygotes at the 1-cell stage rescued expression of *lyz* (Fig. 6D, *n*=21/23), demonstrating an ability for Runx1 to exert function in early myeloid cells (see Discussion). It was not possible to analyze the impact of early *runx1* loss on definitive hematopoiesis in *rad21*^{nz171} because of the developmental arrest by 35 h.p.f.

Cells in *rad21*^{nz171} homozygotes eventually arrest in mitosis with lack of chromosome cohesion

By 48 h.p.f., *rad21*^{nz171} embryos have arrested in development with extensive mitotic defects (Fig. 2G-J). We used immunofluorescence and confocal microscopy to examine cell cycle defects in *rad21*^{nz171} embryos during development. At the 14-somite stage, *rad21*^{nz171} embryos can be identified by greater numbers of pH3^{+} mitotic cells (Fig. 2D). Interestingly, Rad21 protein was still detectable by immunofluorescence in 14-somite *rad21*^{nz171} embryos (Fig. 7A), a stage when *runx1* and *runx3* expression was abrogated. Rad21 was associated with the nuclei of non-mitotic cells, and became displaced from nuclei in M phase (Fig. 7A). Although there were greater numbers of M phase cells in *rad21*^{nz171} embryos (Fig. 2C,D), mitotic cells appeared normal. The increase of M phase cells in *rad21*^{nz171} mutants at this stage probably reflects an increase in the length of time taken for cells to complete mitosis, as the available pool of maternal Rad21 becomes progressively depleted. From 29 h.p.f., Rad21 protein is no longer detected in *rad21*^{nz171} embryos (Fig. 3C). In 48 h.p.f. *rad21*^{nz171} embryos, multiple cells in a field had arrested in mitosis with highly abnormal spindles (Fig. 7B,C). Condensed chromosomes were spread throughout these cells with clumping at the poles (see also Fig. 2H,J). These observations were reiterated in *rad21* morphants (Fig. 7D). Our data are consistent with previous findings that Rad21 function in the cohesin complex is essential for holding sister chromatids together prior to anaphase (Nasmyth and Haering, 2005).

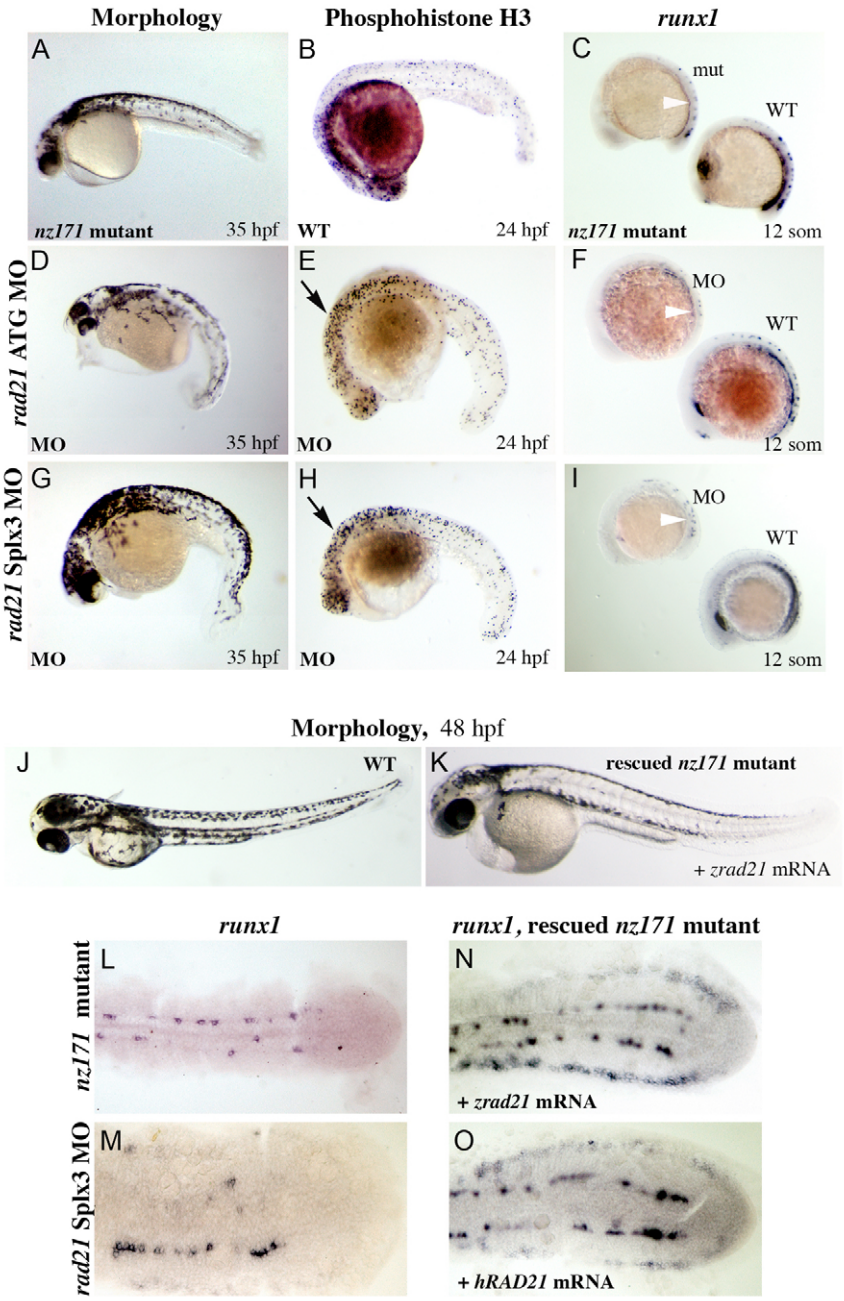

Fig. 4. Morpholino knockdown of the *rad21* gene phenocopies the nz171 mutation, both of which are rescued by injection of *rad21* mRNA. (**A-I**) *rad21* morphants phenocopy the nz171 mutation. (D,G) Embryos injected with antisense morpholino oligonucleotides targeting the start codon (*rad21* ATG MO; D) and 5′ donor site of exon 3 (*rad21* Splx3 MO; G) physically resemble nz171 mutants (example in A) at 35 h.p.f. (B,E,H) pH3-labeled cells in *rad21* morphants (E,H) compared with wild type (B). Morphants exhibit increased numbers of cells in M phase (black arrows). (C,F,I) *runx1* expression in nz171 mutant (C) and *rad21* morphant embryos (F,I), shown alongside wild type (WT, wild type; mut, nz171 mutant; MO, morphant). Reduced PLM *runx1* expression is indicated by white arrowheads. All views lateral, anterior to the left. (**J-O**) The nz171 mutant phenotype is rescued by injection of a *rad21* mRNA. (J,K) The morphology of nz171 mutants approaches wild type in *rad21*-injected embryos. (L-O) Expression of *runx1* in the PLM of flat-mounted 10-somite embryos, anterior to the left, dorsal views. *runx1* expression is absent from the PLM in nz171 (L) and virtually absent in a *rad21* morphant (M). *runx1* expression is rescued in the PLM after injection with zebrafish (N) or human (O) *rad21* mRNA. See Fig. 5, Fig. 6A for wild-type expression of *runx1*.

Intact cohesin is necessary for correct regulation of Runx gene expression

We next asked if Rad21 is operating as part of the cohesin complex in the regulation of Runx gene expression. We used MOs to knock down the function of Smc3, another integral subunit of the cohesin complex (see Fig. S4 in the supplementary material). *smc3* morphants appeared morphologically similar to *rad21* morphants and the *rad21*^{nz171} mutant (see Fig. S4 in the supplementary material). We observed mitotic cells in *smc3* morphants that had condensed chromosomes spread throughout the cell, similar to cells lacking Rad21 (Fig. 7E), indicating a similar role in chromosome cohesion. Lagging chromosomes and ectopic location of chromosomes at the poles were frequently observed. Furthermore, *smc3* morphants lacked early *runx1* and *runx3* expression (Fig. 7F-I). By contrast, a hydroxyurea and aphidicolin S-phase block of the cell cycle had no effect on *runx1* expression (data not shown). Since cells in *rad21*^{nz171} homozygotes successfully complete mitosis at the 14-somite stage, it is unlikely that loss of Runx gene expression at this time is due to a cell cycle block or the activation of cell cycle checkpoints. We therefore believe that the loss of Runx gene expression in *rad21*^{nz171} homozygotes is directly related to a reduction in cohesin. Taken together, our data indicate that the cohesin complex is necessary for normal expression of Runx genes, in addition to its function in sister chromatid cohesion.

Gene expression is dependent on Rad21 dose

Since cells lacking Rad21 cannot divide properly (Sonoda et al., 2001), a maternal complement of *rad21* mRNA or Rad21 protein is likely to sustain proliferation until cells in *rad21*^{nz171} embryos eventually arrest in mitosis on depletion of Rad21 protein. In support of this notion, we found that *rad21* mRNA is maternally inherited

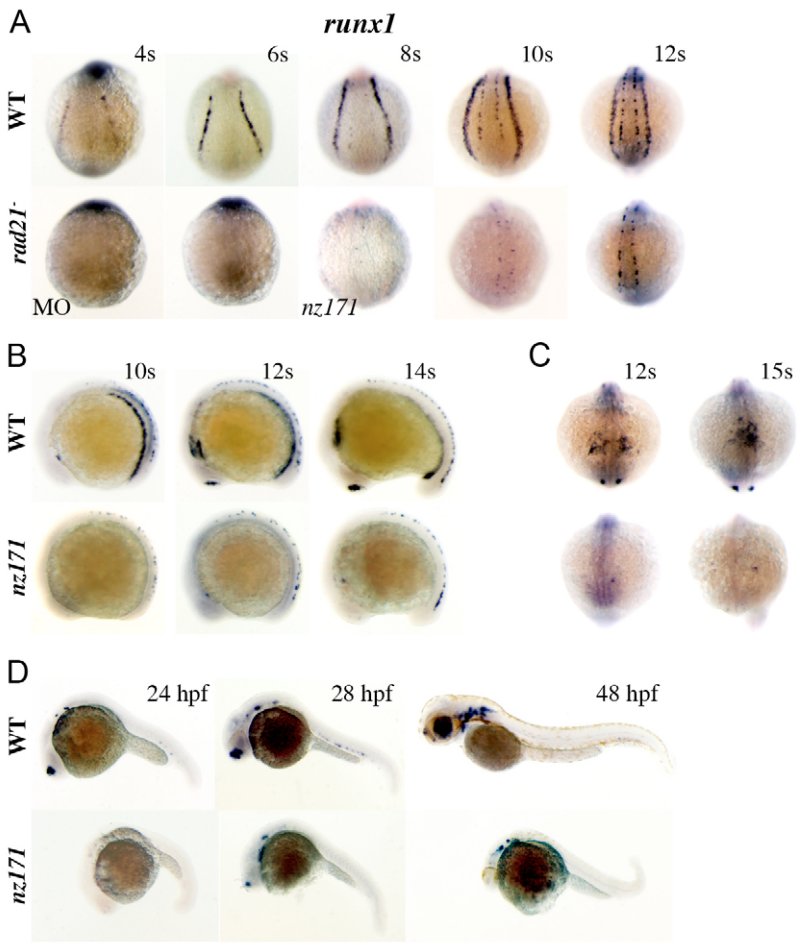

Fig. 5. *runx1* expression fails to initiate in the ALM and PLM of zebrafish embryos compromised for Rad21, but late neuronal *runx1* expression is Rad21-independent. (**A-D**) Whole-mount embryos stained for *runx1* expression. For all, upper panels are wild type, lower panels are *rad21*ATGMO morphants (MO) or nz171 homozygotes as indicated. (A) Posterior views of embryos, stages as indicated. *rad21* morphants (MO; 0.5 pmol) at the 4-somite stage (4s; 14/15 embryos) and 6s (23/25 embryos) were *runx1* negative. Expression of *runx1* in RB cells is just detectable by the 8-somite stage in nz171 mutants, but PLM expression remains absent throughout. (B) Lateral views, stages as indicated. *runx1* mRNA is not detected in the PLM or ICM, or in the olfactory placode of nz171 mutants, but is present in a population of RB cells. (C) Anterior views, stages as indicated. The occasional *runx1*-positive cell is visible in the ALM of nz171 mutants. (D) Lateral views, stages as indicated. At 24 h.p.f., nz171 homozygotes appear delayed and display no *runx1* expression. By 28 h.p.f., neuronal and olfactory placode expression has initiated in mutants. Hematopoietic expression remains absent, c.f. wild type, where expression of *runx1* is observed in the ventral wall of the dorsal aorta. Anterior is to the left for B and D.

(Fig. 3D). Furthermore, Rad21 protein was detected by immunoblotting in 10-somite and 14-somite *rad21*ATGMO morphants, and in 18-somite *rad21*^{nz171} homozygotes (Fig. 8A,B).

If cells in early *rad21*^{nz171} mutants contain Rad21 protein and continue to proliferate (Fig. 7A), but are unable to express *runx1* or *runx3* (Fig. 1G,H, Fig. 5A-C), then the correct regulation of Runx genes might depend on the dose of Rad21 protein. To determine whether Rad21 protein levels change as a result of gene dose, we quantified Rad21 protein in a *rad21*^{nz171} sibling pool (of which two out of three are heterozygotes) in comparison with wild-type embryos. Rad21 protein was reduced by 40% (Fig. 8C) commensurate with a reduction in *rad21* mRNA (Fig. 8D, top left) in *rad21*^{nz171} siblings. Using quantitative RT-PCR, we compared *runx1* expression in *rad21*^{nz171} mutants (–/–) and siblings (+/– and +/+) with wild-type (+/+) embryos at 24 h.p.f. We found that *runx1* transcription is moderately reduced in *rad21*^{nz171} siblings relative to wild-type, with a further reduction in mutants (Fig. 8D, top right). These results indicate that early *runx1* expression is sensitive to changes in the dose of *rad21*. Interestingly, we detected no difference in *runx1* levels between +/+ embryos and *rad21*^{nz171} siblings at 48 h.p.f. (data not shown), indicating that later expression of *runx1* is probably not Rad21-dependent.

rad21^{nz171} homozygotes have defects in neuronal development during early embryogenesis (J.A.H. and J.K-H.H., unpublished) and *rad21* is specifically expressed in restricted regions of the brain at 48 h.p.f. (Fig. 3F). To determine if changes in the dose of *rad21* can affect the expression of neuronal genes in older embryos, we used quantitative RT-PCR to monitor expression of selected neuronal genes in 48 h.p.f. embryos. We found that expression of proneural genes *ascl1a* and *ascl1b*, which are strongly expressed in the brain during embryogenesis (Allende and Weinberg, 1994), was severely reduced in *rad21*^{nz171} mutants and significantly reduced in siblings (Fig. 8D, lower graphs). Our data indicate that although *rad21*^{nz171} siblings appear to grow and develop normally, they are unable to express wild-type levels of downstream genes. This finding points to a regulatory function for cohesin that can be separated from its cell cycle role.

Cohesin contributes to a novel regulatory mechanism for early *runx1* expression

To understand how Rad21/cohesin might influence Runx gene expression, we investigated whether loss of *rad21* affects pathways known to be upstream of *runx1*. The *cdx* (*hox*) pathway specifies blood development from mesoderm, and is essential for *runx1* expression in embryogenesis (Davidson et al., 2003; Davidson and Zon, 2006). We determined that the expression of *cdx4* and its downstream *hox* targets (*hoxa9a*, *hoxb4*, *hoxb6b*, *hoxb7a*) were unaffected in 10-somite *rad21*^{nz171} homozygotes (data not shown). The Notch signaling pathway is upstream of definitive *runx1* expression in zebrafish (Burns et al., 2005). Interestingly, we found that several genes induced by Notch signaling are downregulated in *rad21*^{nz171} embryos (J.A.H. and S.H.A., unpublished results). However, consistent with previous data (Burns et al., 2005; Gering and Patient, 2005), we found that early expression of *runx1* is not Notch dependent (data not shown), thereby eliminating this pathway as an intermediate between cohesin and early *runx1* expression. In

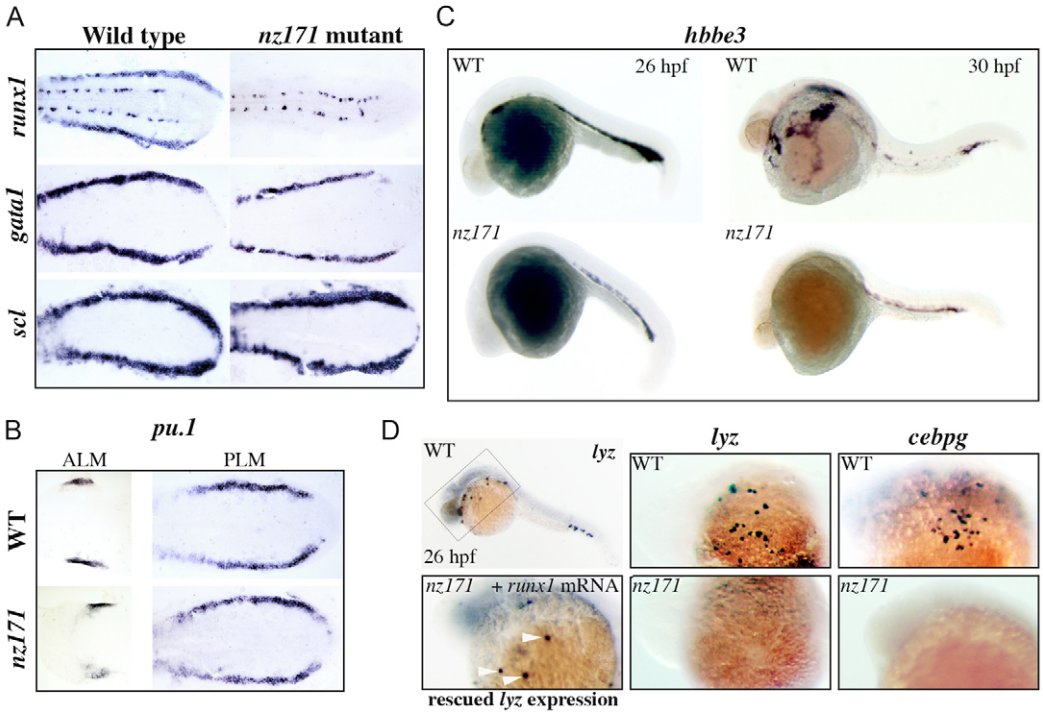

Fig. 6. Expression of genes that mark 'early' versus differentiated hematopoietic cells in zebrafish nz171 mutants, and partial rescue of differentiated cells by microinjection of *runx1* mRNA. (**A**,**B**) Expression of *runx1* and *gata1* is altered in nz171 mutants. Flat preparations of 10-somite embryos, anterior to the left. Expression of *runx1*, *gata1* and *scl* in the PLM (A), and *pu.1* in the ALM and PLM (B) of wild-type siblings and nz171 mutants. *gata1* expression in nz171 mutants is noticeably reduced compared with wild type. (**C**,**D**) Expression of genes that mark differentiated hematopoietic cells is reduced or absent in nz171 mutants. Whole-mount embryos, anterior to the left. (C) Reduced expression of *hbbe3* (*hemoglobin beta embryonic3*) in nz171 mutant embryos (lower panels) compared with wild type (upper panels). (D) Loss of *lyz* (*lysozyme*) expression in nz171 is rescued by microinjection of *runx1* mRNA. Upper left, whole-mount 26 h.p.f. embryo stained for *lyz* expression. The box indicates the region shown at higher magnification in the other panels. Upper panels, wild-type expression of *lyz* and *cebpg* in 26 h.p.f. embryos, as indicated. Lower center and right, similar views of 26 h.p.f. nz171 homozygotes, showing no expression of *lyz* and *cebpg*. Lower left panel, rescued expression of *lyz* in 26 h.p.f. embryos indicated by white arrowheads (21/23 mutant embryos rescued).

summary, two previously characterized pathways shown to contribute to *runx1* expression do not mediate the cohesin regulatory function. Therefore cohesin appears to have a novel role in the regulation of early *runx1* expression.

DISCUSSION

Cohesin specifically regulates early *runx1* expression

The impact of cohesin loss on *runx1* expression appears to be extraordinarily specific. Other zebrafish mutations affecting early *runx1* transcription also perturb the expression of multiple hematopoietic transcription factors (e.g. *spt*, *kgg*) (Hsia and Zon, 2005). Therefore, *rad21*^{nz171} appears to be the first mutant that affects early expression of *runx1* alone. Although most other early hematopoietic markers are expressed normally in *rad21*^{nz171}, early myelopoiesis is deficient and *hbbe3* expression is reduced. By 24 h.p.f., the cell cycle is severely affected in *rad21*^{nz171} (Fig. 2) and therefore hematopoietic progenitors might be unable to divide to form differentiated progeny. In addition, cell death in the ICM almost certainly contributes to a reduction in differentiated cells (Fig. 2L). However, live hematopoietic progenitors remain in the ICM of *rad21*^{nz171} mutants, as indicated by robust *scl* and *gata2* expression at 24 h.p.f.; furthermore, inappropriate maintenance of *scl* expression in the ICM at 48 h.p.f. points to the persistence of immature precursors that cannot differentiate (see Fig. S1 in the supplementary material). Loss of differentiated cells in *rad21*^{nz171} might be due in part to loss of *runx1* and reduction in *gata1* mRNA. Rescue of *lyz*$^{+}$ cells by *runx1* mRNA indicates that either, (1) *runx1* is necessary for early myelopoiesis and its restoration rescues differentiated cells, or (2) expression of *runx1* is able to overcome a developmental block in the myeloid precursors of *rad21*^{nz171} by driving more cells toward a myeloid fate at an earlier time. In support of the latter, we observed an increase in the number of *lyz*$^{+}$ cells in siblings of *runx1*-injected *rad21*^{nz171} crosses (n=41/41, data not shown). Unfortunately, the cell cycle block in *rad21*^{nz171} prevented an analysis of effects on definitive hematopoiesis.

Our results add to increasing evidence that chromatin-modifying proteins can have specific roles in hematopoiesis. In previous studies, a nucleosome assembly protein NAP1L was shown to operate upstream of *scl* in *Xenopus* hematopoiesis (Abu-Daya et al., 2005). Furthermore, Brg1 (a SWI/SNF subunit) appears to have a distinct role in the activation of the β-globin locus in erythropoiesis (Bultman et al., 2005). The involvement of trithorax (Ernst et al., 2004a; Ernst et al., 2004b) and polycomb (Lessard and Sauvageau, 2003; Lessard et al., 1999) group members as epigenetic regulators of hematopoietic stem cell development is relatively well characterized.

A role for cohesin in vertebrate gene regulation

We report the first direct example of cohesin-dependent gene regulation in a vertebrate. Previous studies in *Drosophila* implicated cohesin loading protein, Nipped-B, and cohesin subunits in

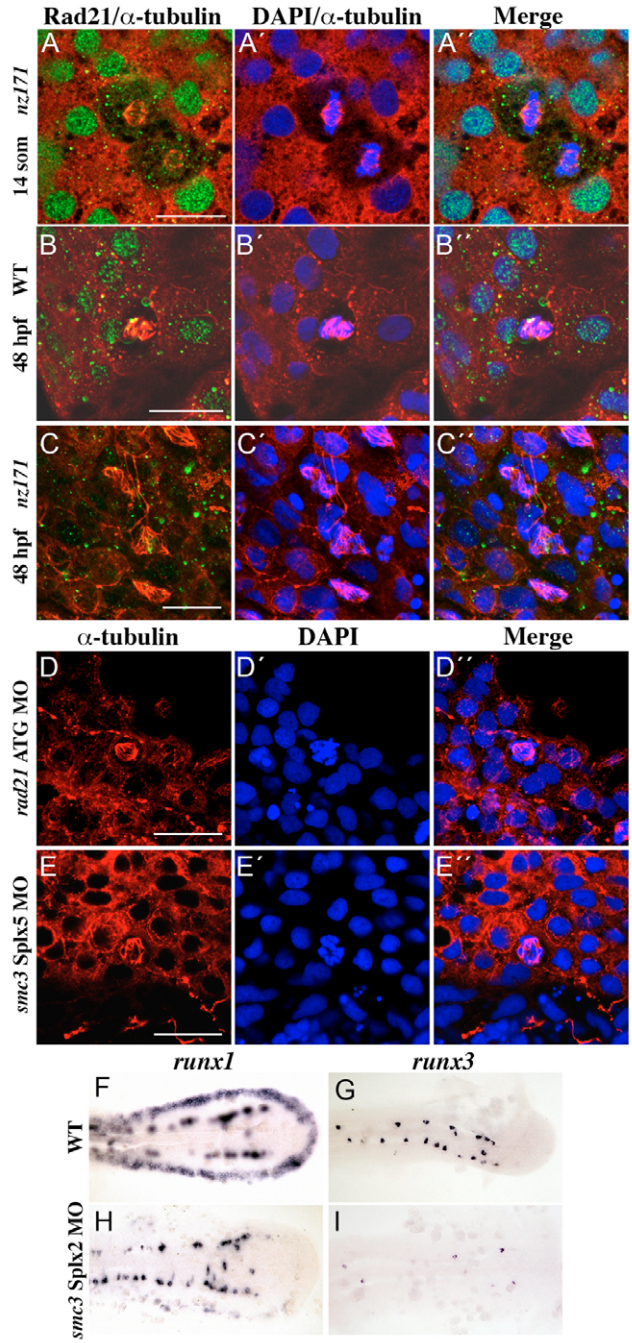

Fig. 7. Zebrafish cohesin functions in sister chromatid cohesion and is necessary for normal expression of Runx genes in early embryogenesis. (**A-C**) Mitotic defects in nz171 embryos. Confocal immunofluorescence images, stained for Rad21 (green) and α-tubulin (red), with DNA stained with DAPI (blue), as indicated on top of the panels; embryo identity is on the left. By 48 h.p.f., Rad21 protein is absent from nz171 embryos, and multiple cells have arrested in mitosis (C-C″). (**D**,**E**) Knocking down the function of Rad21 (D-D″) or Smc3 (E-E″, exon 5 splice site) reproduces the mitotic phenotype observed in nz171 embryos at 48 h.p.f. Confocal immunofluorescence images, stained for α-tubulin (red), with DNA stained with DAPI (blue), as indicated in the panels (top); embryo identity is on the left. For A-E, images are of flat-mounted embryo tails; scale bar is 30 μm. (**F-I**) Loss of *runx1* and *runx3* expression in *smc3* morphants. Flat-mounted 10-somite embryos, anterior to the left. *smc3* morphants (exon 2 splice site) show loss of *runx1* expression in the PLM (H), and *runx3* expression in the RB cells (I).

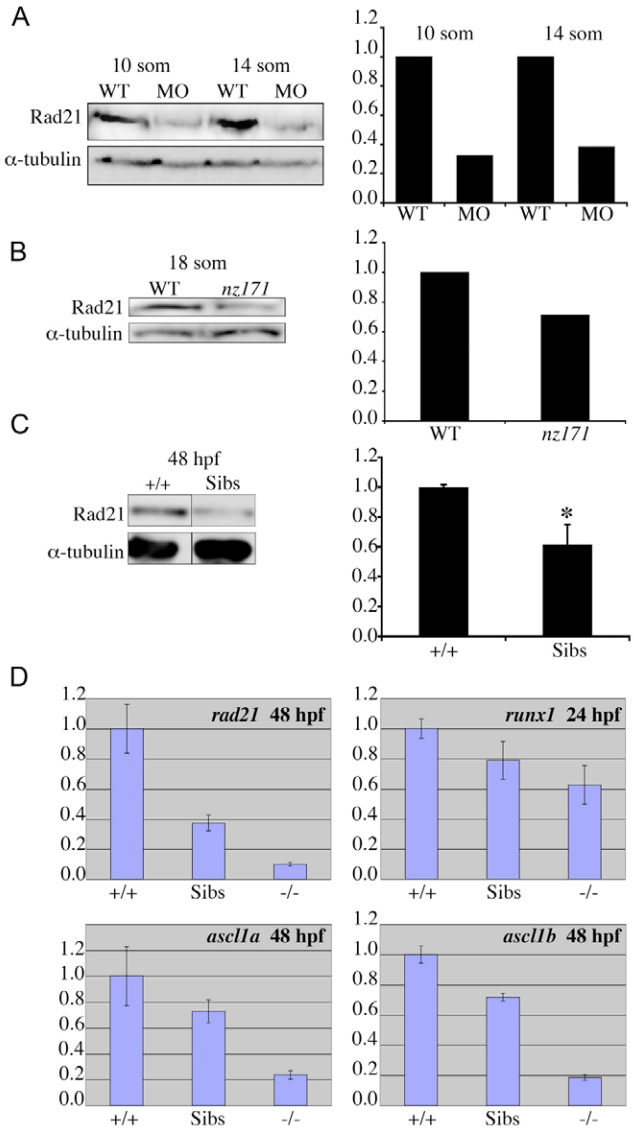

Fig. 8. Maternally inherited Rad21 protein can sustain further cell division, but not gene expression; loss of one copy of *rad21* affects transcription of *runx1*, *ascl1a* and *ascl1b*. (**A**,**B**) Rad21 protein is detectable in early *rad21* morphant and mutant zebrafish embryos at stages when gene expression is compromised, but cell division can still occur. Protein was isolated from wild-type embryos and *rad21*ATGMO morphants (A) or nz171 homozygotes (B) at the stages indicated. Protein quantities were assessed by immunoblotting, with levels relative to α-tubulin. The graphs on the right show quantification of the immunoblots on the left. (**C**,**D**) Loss of one copy of *rad21* reduces *rad21* transcript and protein levels, and affects gene expression. (C) Protein was isolated from nz171 siblings (Sibs: includes +/+ and +/– embryos, which are phenotypically indistinguishable) and wild-type (+/+) controls at 48 h.p.f. Relative levels of Rad21 protein in nz171 siblings and wild-type embryos were quantified by immunoblotting and results are presented in the graph on the right (values represent the mean±s.e.m. of three independent experiments performed in triplicate. **P*<0.01, Student's *t*-test). A representative immunoblot appears on the left. (D) Quantitative RT-PCR of cDNA generated from pooled wild-type (+/+), nz171 sibling (Sibs) and nz171 mutant (–/–) embryos. Bar charts are representative results from three independent experiments. Values are relative to wild type, bars represent the mean of samples run in triplicate; all values are significant with *P*<0.05.

regulation of the *cut* and *Ultrabithorax* loci (Dorsett et al., 2005; Rollins et al., 1999). In *C. elegans*, the cohesin-loading factor MAU-2 (the Scc4 ortholog) is essential for axon migration during development (Seitan et al., 2006). Our observations of neuronal abnormalities and altered neuronal gene expression in *rad21*^{nz171} embryos, together with the *C. elegans* data, are consistent with the idea that chromosome cohesion proteins have specific roles in neuronal development.

Significantly, we uncovered a potent dose effect of Rad21 levels on gene expression (Fig. 8). Our results raise the possibility that there is a threshold level of Rad21, below which cell proliferation can be sustained, but gene expression is compromised. Perhaps the mitotic function of cohesin is prioritized at the expense of its alternative (potentially regulatory) functions in a depleted cohesin pool.

Linking cohesin function and Runx gene regulation

It is tempting to speculate that loss of early *runx1* and *runx3* expression in *rad21*^{nz171} is causally related to the connection between the Runx family and the cell cycle. Runx protein levels are dynamically regulated during the cell cycle; e.g. expression of *Runx2* oscillates during the cell cycle of MC3T3 osteoblasts (Galindo et al., 2005). In cell lines, Runx1 levels were also shown to oscillate in a cell cycle-dependent manner: Runx1 protein levels increase during S phase and G2 (Bernardin-Fried et al., 2004) and at the G2-M phase transition, Runx1 is degraded by the anaphase-promoting complex (Biggs et al., 2006; Wang et al., 2006). Cohesin becomes stably associated with chromatin during S and G2 (Gerlich et al., 2006), and perhaps this is necessary for *runx1* expression in a particular developmental context. Runx1 degradation is also concomitant with cohesin cleavage at G2-M.

Runx proteins appear to have cell cycle-specific functions. Overexpression of *Runx1* causes a shortening of G1 phase (Strom et al., 2000) and Runx1 physically interacts with cyclin D3 to repress its own transcription (Peterson et al., 2005). During mitosis, Runx2 selectively regulates specific target genes (Young et al., 2007b), and represses transcription of ribosomal RNA genes (Young et al., 2007a). These authors also reported similar unpublished observations for Runx1. Therefore, Runx proteins might regulate cell growth through control of ribosome biogenesis, and it was proposed that by this mechanism Runx proteins might coordinate cell proliferation and differentiation. Clearly, Runx proteins provide a mechanistic link between the cell cycle and development. Therefore a mechanism by which Runx gene expression is coordinated with the cell cycle would make sense. Cohesin is an integral part of the cell cycle machinery, and is therefore a good candidate to participate in cell cycle-dependent gene regulation.

Cohesin-dependent gene regulation and the implications for development

There are a number of human developmental disorders associated with loss of sister chromatid cohesion, including CdLS (Krantz et al., 2004; Musio et al., 2006; Strachan, 2005). This raises the interesting possibility that such developmental disorders might be contributed to by a reduction in Runx gene expression in embryogenesis, as a result of reduction in cohesin function. CdLS patients present with neurodevelopmental, gastrointestinal and skeletal abnormalities (Strachan, 2005). The development of each of these systems depends on the proper regulation of Runx proteins, which are themselves dose-sensitive in function (Blyth et al., 2005). In summary, our findings provide strong evidence for a novel developmental function for cohesin. The next challenge will be to determine exactly how cohesin contributes to regulation of gene expression and developmental pathways.

The authors thank Wendy Flühler for excellent technical assistance, Anassuya Ramachandran for help with quantitative PCR, Alhad Mahagaonkar and Peter Cattin for zebrafish husbandry, and Latifa Khan for help with screening the F1. We also thank Debbie Yelon, Didier Stainier, Joan Heath and members of the Stainier, Heath and Lieschke laboratories for screening and mapping advice, and Helena Richardson for critical reading of the manuscript. This work was supported by Health Research Council of New Zealand grant 04/120 to P.S.C., J.A.H., and K.E.C.

Supplementary material

Supplementary material for this article is available at http://dev.biologists.org/cgi/content/full/134/14/2639/DC1

References

Abu-Daya, A., Steer, W. M., Trollope, A. F., Friedeberg, C. E., Patient, R. K., Thorne, A. W. and Guille, M. J. (2005). Zygotic nucleosome assembly protein-like 1 has a specific, non-cell autonomous role in hematopoiesis. *Blood* **106**, 514-520.

Allende, M. L. and Weinberg, E. S. (1994). The expression pattern of two zebrafish achaete-scute homolog (ash) genes is altered in the embryonic brain of the cyclops mutant. *Dev. Biol.* **166**, 509-530.

Amsterdam, A., Nissen, R. M., Sun, Z., Swindell, E. C., Farrington, S. and Hopkins, N. (2004). Identification of 315 genes essential for early zebrafish development. *Proc. Natl. Acad. Sci. USA* **101**, 12792-12797.

Bernardin-Fried, F., Kummalue, T., Leijen, S., Collector, M. I., Ravid, K. and Friedman, A. D. (2004). AML1/RUNX1 increases during G1 to S cell cycle progression independent of cytokine-dependent phosphorylation and induces cyclin D3 gene expression. *J. Biol. Chem.* **279**, 15678-15687.

Biggs, J. R., Peterson, L. F., Zhang, Y., Kraft, A. S. and Zhang, D. E. (2006). AML1/RUNX1 phosphorylation by cyclin-dependent kinases regulates the degradation of AML1/RUNX1 by the anaphase-promoting complex. *Mol. Cell. Biol.* **26**, 7420-7429.

Blyth, K., Cameron, E. R. and Neil, J. C. (2005). The RUNX genes: gain or loss of function in cancer. *Nat. Rev. Cancer* **5**, 376-387.

Bultman, S. J., Gebuhr, T. C. and Magnuson, T. (2005). A Brg1 mutation that uncouples ATPase activity from chromatin remodeling reveals an essential role for SWI/SNF-related complexes in beta-globin expression and erythroid development. *Genes Dev.* **19**, 2849-2861.

Burns, C. E., Traver, D., Mayhall, E., Shepard, J. L. and Zon, L. I. (2005). Hematopoietic stem cell fate is established by the Notch-Runx pathway. *Genes Dev.* **19**, 2331-2342.

Chang, Y. F., Imam, J. S. and Wilkinson, M. F. (2007). The nonsense-mediated decay RNA surveillance pathway. *Annu. Rev. Biochem.* **76** (in press).

Davidson, A. J. and Zon, L. I. (2006). The caudal-related homeobox genes cdx1a and cdx4 act redundantly to regulate hox gene expression and the formation of putative hematopoietic stem cells during zebrafish embryogenesis. *Dev. Biol.* **292**, 506-518.

Davidson, A. J., Ernst, P., Wang, Y., Dekens, M. P., Kingsley, P. D., Palis, J., Korsmeyer, S. J., Daley, G. Q. and Zon, L. I. (2003). cdx4 mutants fail to specify blood progenitors and can be rescued by multiple hox genes. *Nature* **425**, 300-306.

Dorsett, D. (2007). Roles of the sister chromatid cohesion apparatus in gene expression, development, and human syndromes. *Chromosoma* **116**, 1-13.

Dorsett, D., Eissenberg, J. C., Misulovin, Z., Martens, A., Redding, B. and McKim, K. (2005). Effects of sister chromatid cohesion proteins on cut gene expression during wing development in *Drosophila*. *Development* **132**, 4743-4753.

Elagib, K. E., Racke, F. K., Mogass, M., Khetawat, R., Delehanty, L. L. and Goldfarb, A. N. (2003). RUNX1 and GATA-1 coexpression and cooperation in megakaryocytic differentiation. *Blood* **101**, 4333-4341.

Ernst, P., Fisher, J. K., Avery, W., Wade, S., Foy, D. and Korsmeyer, S. J. (2004a). Definitive hematopoiesis requires the mixed-lineage leukemia gene. *Dev. Cell* **6**, 437-443.

Ernst, P., Mabon, M., Davidson, A. J., Zon, L. I. and Korsmeyer, S. J. (2004b). An Mll-dependent Hox program drives hematopoietic progenitor expansion. *Curr. Biol.* **14**, 2063-2069.

Galindo, M., Pratap, J., Young, D. W., Hovhannisyan, H., Im, H. J., Choi, J. Y., Lian, J. B., Stein, J. L., Stein, G. S. and van Wijnen, A. J. (2005). The bone-specific expression of Runx2 oscillates during the cell cycle to support a G1-related antiproliferative function in osteoblasts. *J. Biol. Chem.* **280**, 20274-20285.

Geisler, R. (2002). Mapping and cloning. In *Zebrafish, A Practical Approach*. Vol. 261 (ed. C. Nusslein-Volhard and R. Dahm), pp. 175-212. Oxford: Oxford University Press.

Gering, M. and Patient, R. (2005). Hedgehog signaling is required for adult blood stem cell formation in zebrafish embryos. *Dev. Cell* **8**, 389-400.
Gerlich, D., Koch, B., Dupeux, F., Peters, J.-M. and Ellenberg, J. (2006). Live-cell imaging reveals a stable cohesin-chromatin interaction after but not before DNA replication. *Curr. Biol.* **16**, 1571-1578.
Hagstrom, K. A. and Meyer, B. J. (2003). Condensin and cohesin: more than chromosome compactor and glue. *Nat. Rev. Genet.* **4**, 520-534.
Hsia, N. and Zon, L. I. (2005). Transcriptional regulation of hematopoietic stem cell development in zebrafish. *Exp. Hematol.* **33**, 1007-1014.
Ito, Y. (2004). Oncogenic potential of the RUNX gene family: 'overview'. *Oncogene* **23**, 4198-4208.
Kalev-Zylinska, M. L., Horsfield, J. A., Flores, M. V., Postlethwait, J. H., Vitas, M. R., Baas, A. M., Crosier, P. S. and Crosier, K. E. (2002). Runx1 is required for zebrafish blood and vessel development and expression of a human RUNX1-CBF2T1 transgene advances a model for studies of leukemogenesis. *Development* **129**, 2015-2030.
Kalev-Zylinska, M. L., Horsfield, J., Flores, M. V., Postlethwait, J., Chau, J. Y. M., Cattin, P. M., Vitas, M. R., Crosier, P. S. and Crosier, K. E. (2003). Runx3 is required for hematopoietic development in zebrafish. *Dev. Dyn.* **228**, 323-336.
Kobayashi, M., Nishikawa, K. and Yamamoto, M. (2001). Hematopoietic regulatory domain of gata1 gene is positively regulated by GATA1 protein in zebrafish embryos. *Development* **128**, 2341-2350.
Krantz, I. D., McCallum, J., DeScipio, C., Kaur, M., Gillis, L. A., Yaeger, D., Jukofsky, L., Wasserman, N., Bottani, A., Morris, C. A. et al. (2004). Cornelia de Lange syndrome is caused by mutations in NIPBL, the human homolog of Drosophila melanogaster Nipped-B. *Nat. Genet.* **36**, 631-635.
Lau, Q. C., Raja, E., Salto-Tellez, M., Liu, Q., Ito, K., Inoue, M., Putti, T. C., Loh, M., Ko, T. K., Huang, C. et al. (2006). RUNX3 is frequently inactivated by dual mechanisms of protein mislocalization and promoter hypermethylation in breast cancer. *Cancer Res.* **66**, 6512-6520.
Lessard, J. and Sauvageau, G. (2003). Polycomb group genes as epigenetic regulators of normal and leukemic hemopoiesis. *Exp. Hematol.* **31**, 567-585.
Lessard, J., Schumacher, A., Thorsteinsdottir, U., van Lohuizen, M., Magnuson, T. and Sauvageau, G. (1999). Functional antagonism of the Polycomb-Group genes eed and Bmi1 in hemopoietic cell proliferation. *Genes Dev.* **13**, 2691-2703.
Losada, A. and Hirano, T. (2005). Dynamic molecular linkers of the genome: the first decade of SMC proteins. *Genes Dev.* **19**, 1269-1287.
Mueller, W., Nutt, C. L., Ehrich, M., Riemenschneider, M. J., von Deimling, A., van den Boom, D. and Louis, D. N. (2007). Downregulation of RUNX3 and TES by hypermethylation in glioblastoma. *Oncogene* **26**, 583-593.
Musio, A., Selicorni, A., Focarelli, M. L., Gervasini, C., Milani, D., Russo, S., Vezzoni, P. and Larizza, L. (2006). X-linked Cornelia de Lange syndrome owing to SMC1L1 mutations. *Nat. Genet.* **38**, 528-530.
Nakagawa, M., Ichikawa, M., Kumano, K., Goyama, S., Kawazu, M., Asai, T., Ogawa, S., Kurokawa, M. and Chiba, S. (2006). AML1/Runx1 rescues Notch1-Null mutation-induced deficiency of para-aortic splanchnopleural hematopoiesis. *Blood* **108**, 3329-3334.
Nasmyth, K. and Haering, C. H. (2005). The structure and function of SMC and kleisin complexes. *Annu. Rev. Biochem.* **74**, 595-648.
Patterson, L. J., Gering, M. and Patient, R. (2005). Scl is required for dorsal aorta as well as blood formation in zebrafish embryos. *Blood* **105**, 3502-3511.
Patterson, L. J., Gering, M., Eckfeldt, C. E., Green, A. R., Verfaillie, C. M., Ekker, S. C. and Patient, R. (2007). The transcription factors Scl and Lmo2 act together during development of the hemangioblast in zebrafish. *Blood* **109**, 2389-2398.
Pelegri, F. (2002). Mutagenesis. In *Zebrafish, A Practical Approach*. Vol. 261 (ed. C. Nusslein-Volhard and R. Dahm), pp. 145-174. Oxford: Oxford University Press.
Peterson, L. F., Boyapati, A., Ranganathan, V., Iwama, A., Tenen, D. G., Tsai, S. and Zhang, D. E. (2005). The hematopoietic transcription factor AML1 (RUNX1) is negatively regulated by the cell cycle protein cyclin D3. *Mol. Cell. Biol.* **25**, 10205-10219.
Pimanda, J. E., Donaldson, I. J., de Bruijn, M. F., Kinston, S., Knezevic, K., Huckle, L., Piltz, S., Landry, J. R., Green, A. R., Tannahill, D. et al. (2007). The SCL transcriptional network and BMP signaling pathway interact to regulate RUNX1 activity. *Proc. Natl. Acad. Sci. USA* **104**, 840-845.
Rollins, R. A., Morcillo, P. and Dorsett, D. (1999). Nipped-B, a Drosophila homologue of chromosomal adherins, participates in activation by remote enhancers in the cut and Ultrabithorax genes. *Genetics* **152**, 577-593.
Rollins, R. A., Korom, M., Aulner, N., Martens, A. and Dorsett, D. (2004). Drosophila nipped-B protein supports sister chromatid cohesion and opposes the stromalin/Scc3 cohesion factor to facilitate long-range activation of the cut gene. *Mol. Cell. Biol.* **24**, 3100-3111.
Seitan, V. C., Banks, P., Laval, S., Majid, N. A., Dorsett, D., Rana, A., Smith, J., Bateman, A., Krpic, S., Hostert, A. et al. (2006). Metazoan Scc4 homologs link sister chromatid cohesion to cell and axon migration guidance. *PLoS Biol.* **4**, e242.
Shepard, J., Stern, H. M., Pfaff, K. L. and Amatruda, J. F. (2004). Analysis of the cell cycle in Zebrafish embryos. In *The Zebrafish: Cellular and Developmental Biology.* Vol. 76, 2nd edn (ed. H. W. Detrich, 3rd, M. Westerfield and L. Zon), pp. 109-125. San Diego: Elsevier.
Sonoda, E., Matsusaka, T., Morrison, C., Vagnarelli, P., Hoshi, O., Ushiki, T., Nojima, K., Fukagawa, T., Waizenegger, I. C., Peters, J. M. et al. (2001). Scc1/Rad21/Mcd1 is required for sister chromatid cohesion and kinetochore function in vertebrate cells. *Dev. Cell* **1**, 759-770.
Strachan, T. (2005). Cornelia de Lange Syndrome and the link between chromosomal function, DNA repair and developmental gene regulation. *Curr. Opin. Genet. Dev.* **15**, 258-264.
Strom, D. K., Nip, J., Westendorf, J. J., Linggi, B., Lutterbach, B., Downing, J. R., Lenny, N. and Hiebert, S. W. (2000). Expression of the AML-1 oncogene shortens the G(1) phase of the cell cycle. *J. Biol. Chem.* **275**, 3438-3445.
Waltzer, L., Ferjoux, G., Bataille, L. and Haenlin, M. (2003). Cooperation between the GATA and RUNX factors Serpent and Lozenge during Drosophila hematopoiesis. *EMBO J.* **22**, 6516-6525.
Wang, S., Zhang, Y., Soosairajah, J. and Kraft, A. S. (2006). Regulation of RUNX1/AML1 during the G2/M transition. *Leuk. Res.* doi:10.1016/j.leukres.2006.08.016.
Watrin, E. and Peters, J. M. (2006). Cohesin and DNA damage repair. *Exp. Cell Res.* **312**, 2687-2693.
Westerfield, M. (1995). *The Zebrafish Book. A Guide for the Laboratory Use of Zebrafish (Danio rerio).* Eugene, OR: University of Oregon Press.
Woods, I. G., Kelly, P. D., Chu, F., Ngo-Hazelett, P., Yan, Y. L., Huang, H., Postlethwait, J. H. and Talbot, W. S. (2000). A comparative map of the zebrafish genome. *Genome Res.* **10**, 1903-1914.
Young, D. W., Hassan, M. Q., Pratap, J., Galindo, M., Zaidi, S. K., Lee, S. H., Yang, X., Xie, R., Javed, A., Underwood, J. M. et al. (2007a). Mitotic occupancy and lineage-specific transcriptional control of rRNA genes by Runx2. *Nature* **445**, 442-446.
Young, D. W., Hassan, M. Q., Yang, X. Q., Galindo, M., Javed, A., Zaidi, S. K., Furcinitti, P., Lapointe, D., Montecino, M., Lian, J. B. et al. (2007b). Mitotic retention of gene expression patterns by the cell fate-determining transcription factor Runx2. *Proc. Natl. Acad. Sci. USA* **104**, 3189-3194.